Theoretical Study of Thermally Stable Large-Coupling Lithium Niobate SH_0 Plate Wave Resonator

Jie Zou*, Shuxian Wu*, Zonglin Wu, and Yaqiu Jin
MOE, Fudan University
Shanghai, China
*E-mail: jiezou@fudan.edu.cn, sxwu20@fudan.edu.cn

Albert P. Pisano
Department of Mechanical Engineering,
University of California at Berkeley
Berkeley, USA

***Abstract*—The thermal stabilization techniques for the fundamental (SH_0) Plate acoustic wave (PAW) resonators based on $LiNbO_3$ are theoretically investigated in this paper. The SH_0 mode offers an ultra-large coupling coefficient (k^2) at a certain crystal cut angle and normalized plate thickness, but its poor temperature coefficient of frequency (*TCF*) hinders its application in RF systems and needs further improvement urgently. By adding SiO_2 with positive *TCF* to the $LiNbO_3$ plate, a robust temperature compensation approach can be achieved for the SH_0 resonators on $LiNbO_3/SiO_2$ bilayer and $SiO_2/LiNbO_3/SiO_2$ sandwiched structures. The propagation characteristics of the SH_0 wave propagating in the layered medium are carefully investigated. Despite the trade-off between *TCF* and k^2, the $SiO_2/LiNbO_3/SiO_2$ structure provides large k^2 and near-zero *TCF* for wider thickness combinations. Furthermore, the periodic structure dispersion of the simplest zero-*TCF* stack is provided and the critical threshold IDT thickness is given.**

Keywords*—Lithium Niobate ($LiNbO_3$), piezoelectricity, resonators, plate wave, temperature coefficient of frequency (TCF), thermal stability.

I. Introduction

In response to the drastically increasing demands for ubiquitous wireless connectivity, faster data delivery in wireless mobile, Internet-of-Things (IoT), autonomous vehicles, and artificial intelligence, new services currently go into operation requiring progressively wider frequency bands. The coupling coefficient (k^2) of the commercially popular surface acoustic wave (SAW) or bulk acoustic wave (BAW) technology is between 6%-13%, limiting the filter bandwidth (*BW*) to up to 6%. Both the current bands wider than 6% with tight specifications and the ultra-wide band (> 15%) required by the next-generation re-configurable filters and cognitive radios point the urgent need of micro-acoustic resonators with ultra-large k^2 [1]-[3].

A $LiNbO_3$ plate based SH_0 Plate Acoustic Wave (PAW) resonator characterizes the largest k^2 among all acoustic wave devices, up to 50% in certain cut angles and $LiNbO_3$ thickness [1]. As a result, the SH_0 PAW technology can be an excellent solution to the ultra-wide bands, as well as recently proposed XBARs [4]. However, $LiNbO_3$ features a material property of drastically softening when temperature rises, leading to very poor temperature coefficient of frequency (*TCF*) of ~ -70 ppm/˚C. This poor *TCF* would be unacceptable for any application in current or future RF systems. So an improvement of the thermal stability of $LiNbO_3$-based SH_0 resonators is highly desirable for enabling low-temperature-drift and ultra-wide-band filters [5].

The thermal stability can be achieved by adding SiO_2, which has a positive *TCF* of ~ +80 ppm/˚C to the $LiNbO_3$ plate, forming a robust p assive compensation. The SH_0 wave propagation characteristics are carefully investigated after

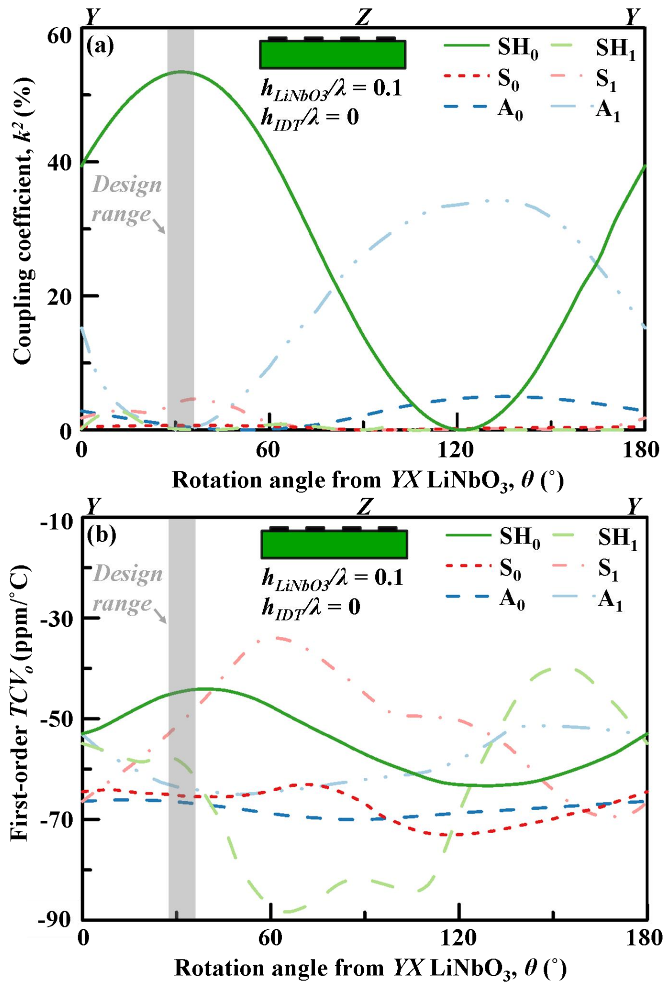

Fig. 1. Calculated (a) phase velocity and (b) first-order *TCV* versus rotation angle of the first six Plate modes in the rotated *YX* $LiNbO_3$ membrane (h_{LiNbO3}/λ=0.1) when the mechanical loading of IDT is ignored (h_{IDT}=0).

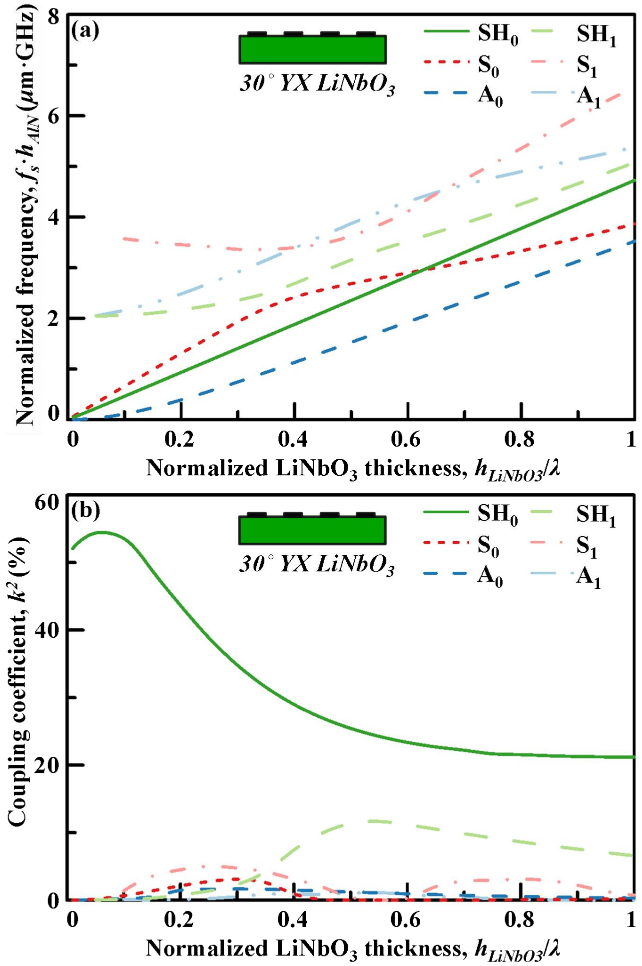

Fig. 2. Calculated (a) *f*-*β* dispersion curve and (b) dispersive k^2 of the first six Plate modes in the 30° *YX* $LiNbO_3$ membrane ($h_{IDT} = 0$).

introducing the non-piezoelectric SiO_2 herein and optimized stack proposed for achieving the thermal insensitivity and large k^2 simultaneously. Moreover, the periodic structure dispersion of the simplest zero-*TCF* stack is provided.

II. SH_0 Plate Wave in $LiNbO_3$

A. Cut Angle

Fig. 1 (a) and (b) show the k^2 and temperature coefficient of velocity (*TCV*) across all rotation angle from the *YX* $LiNbO_3$ for the first six Plate modes with $h_{LiNbO3}/\lambda = 0.1$ (λ is twice the IDT pitch). The k^2 varies largely due to the prominent anisotropy of the piezoelectric matrix, so the optimal cut angle can be chosen so as to optimize the k^2. The peak k^2 of 55% happens at rotation angle of ~30° with Euler angle (0°,120°,0°). It is also interesting to note that at this rotation angle of around 30°, the k^2's of most other Plate modes are minimized, especially the A_1 Lamb mode that is outstanding around *Z*-cut.

The *TCV* can be derived from the temperature coefficients of elasticities (*TCE*'s) and temperature dependence of density of $LiNbO_3$ [7]. By adding the effect of *TCV* together with the thermal expansion coefficient (α), *TCF* can be estimated as:

$$TCF_{1st} = \frac{1}{f}\frac{\partial f}{T} = \frac{1}{v}\frac{\partial v}{T} - \alpha_x = TCV_{1st} - \alpha_x \quad (1)$$

The α_x of $LiNbO_3$ is around 15.4 ppm/°C so that the $LiNbO_3$ plate based resonators show very poor intrinsic *TCF* of -60—100 ppm/°C. Luckily at the rotation angle of ~ 30° the *TCV* of the SH_0 mode is minimized across the entire cut angle.

B. Dispersion

The dispersion characteristics of the first six Plate waves propagating in the 30° *YX* $LiNbO_3$ with h_{LiNbO3}/λ =0.1 are shown in Fig. 2 (a). The normalized wave number of the *x* axis corresponds to normalized $LiNbO_3$ plate thickness:

$$\frac{\beta \cdot h_{LiNbO3}}{2\pi} = \frac{h_{LiNbO3}}{\lambda}. \quad (2)$$

Evidently, the SH_0 mode shows weakest dispersion and features the advantage of pitch-controlled frequency even when the $LiNbO_3$ plate thickness approaches zero. In addition, the low dispersion of the fundamental modes also allows the agile design of the acoustic-coupled filters [6].

Fig. 2 (b) depicts the dispersive k^2 of the first six Plate waves for the single-IDT transducer configuration in the 30° *YX* $LiNbO_3$. At this cut angle of (0°,120°,0°), the SH_0 mode features very large k^2 while the other modes are suppressed. Especially when $LiNbO_3$ is thin (< 0.2λ), the k^2 is higher than 40% and clean wide-band spectrum is expected.

III. SH_0 Wave Characteristics in $LiNbO_3/SiO_2$ and $SiO_2/LiNbO_3/SiO_2$

A. Phase Velocity Degradation

The piezoelectric-dead SiO_2 layer loads the $LiNbO_3$ thin film and significantly reduces the phase velocity (v_p) of the SH_0 mode in the $LiNbO_3/SiO_2$ membrane, as shown in Fig. 3. The v_p of the SH_0 mode in the symmetrical $SiO_2/LiNbO_3/SiO_2$ membrane is higher than that in the $LiNbO_3/SiO_2$ bilayer structure, especially when the thicker SiO_2 layer is utilized and h_{LiNbO3}/λ is small. At thin $LiNbO_3$ with h_{LiNbO3}/λ =0.1 the SH_0 mode in the $SiO_2/LiNbO_3/SiO_2$ membrane shows the phase velocity of roughly 4,280 m/s and in the $LiNbO_3/SiO_2$ bilayer

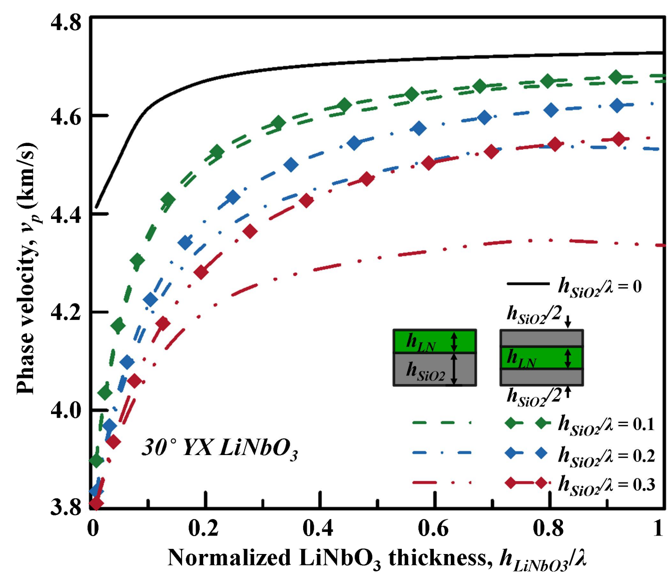

Fig. 3. Comparison of the FEA simulated v_p dispersion of the SH_0 mode in the $LiNbO_3/SiO_2$ bilayer membrane and in the symmetrical $SiO_2/LiNbO_3/SiO_2$ composite membrane with 30° *YX* $LiNbO_3$.

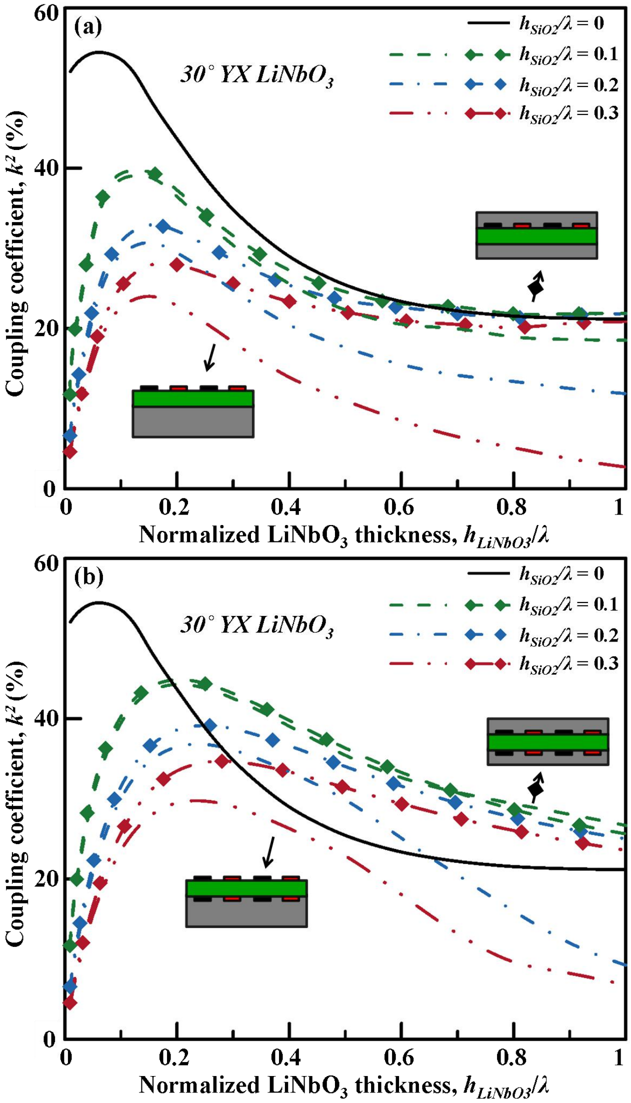

Fig. 4. Comparison of the FEA simulated k^2 dispersion utilizing the SH_0 mode in the $LiNbO_3/SiO_2$ bilayer membrane and in the symmetrical $SiO_2/LiNbO_3/SiO_2$ composite membrane with (a) single-IDT and (b) double-IDT.

structure around 4,200 m/s at $h_{SiO2}/\lambda = 0.2$.

B. Coupling Coefficient Degradation

As depicted in Fig. 4, the k^2 dispersion curves of the SH_0 mode on the $LiNbO_3/SiO_2$ and $SiO_2/LiNbO_3/SiO_2$ composite membrane are compared with single-IDT and double-IDT transducer configurations. The k^2 is usually deteriorated by the additional SiO_2 layer because of the acoustic energy absorption by the piezo-dead and soft SiO_2 layer. Since the acoustic wave field tends to be more involved in the $LiNbO_3$ layer of the symmetrical $SiO_2/LiNbO_3/SiO_2$ plate, the acoustic energy can be confined in the $LiNbO_3$ plate to enable a higher k^2 for the SH_0 mode. As a result, especially when thick SiO_2 layers are employed, the k^2 of the SH_0 mode in the $SiO_2/LiNbO_3/SiO_2$ sandwiched plate is larger than in the $LiNbO_3/SiO_2$.

Intriguingly, for some cases the k^2 of the SH_0 mode in the layered plates can be even larger than that in the $LiNbO_3$ single plate. For example when $h_{LiNbO3}/\lambda = 0.3–1$ is employed for double-IDT and double-SiO_2, the k^2 is much increased, where the growing contribution of the e_{15} piezoelectric constant by the surface constraint overcomes the loading effect.

C. TCF and Trade-Off

Neglecting the electrode thickness, the first-order *TCF*'s of the $LiNbO_3/SiO_2$ and $SiO_2/LiNbO_3/SiO_2$ SH_0 resonators can be theoretically predicted and are depicted in dashed lines of Fig. 5 and Fig. 6. By adding the SiO_2 layers onto the $LiNbO_3$ thin film, the *TCF*'s increase fast and cross 0 ppm/C°. However, the first-order *TCF*'s in the $SiO_2/LiNbO_3/SiO_2$ plate are slightly smaller than in the $LiNbO_3/SiO_2$ plate at the same h_{LiNbO3}/λ and h_{SiO2}/λ, giving opposite preference for selecting stack configuration from considering v_p and k^2. In addition, there is also a general trade-off relation between the *TCF* and k^2 for selecting the stack thicknesses.

In order to compare the trade-offs, the k^2 values at zero *TCF* are identified and marked in dots in Fig. 5 and Fig.6. In general, the SH_0 mode in the sandwiched structure still offers a slightly larger k^2 than in the bilayer plate, especially at greater $LiNbO_3$ thicknesses. The simplest zero-*TCF* stack can be $LiNbO_3/SiO_2$ with $h_{LiNbO3}/\lambda = 0.1$, $h_{SiO2}/\lambda = 0.2$, and single-IDT. It is also interesting to notice that for double-IDT and double-SiO_2 the k^2 can be large (~30%) even at a thicker $LiNbO_3$ at

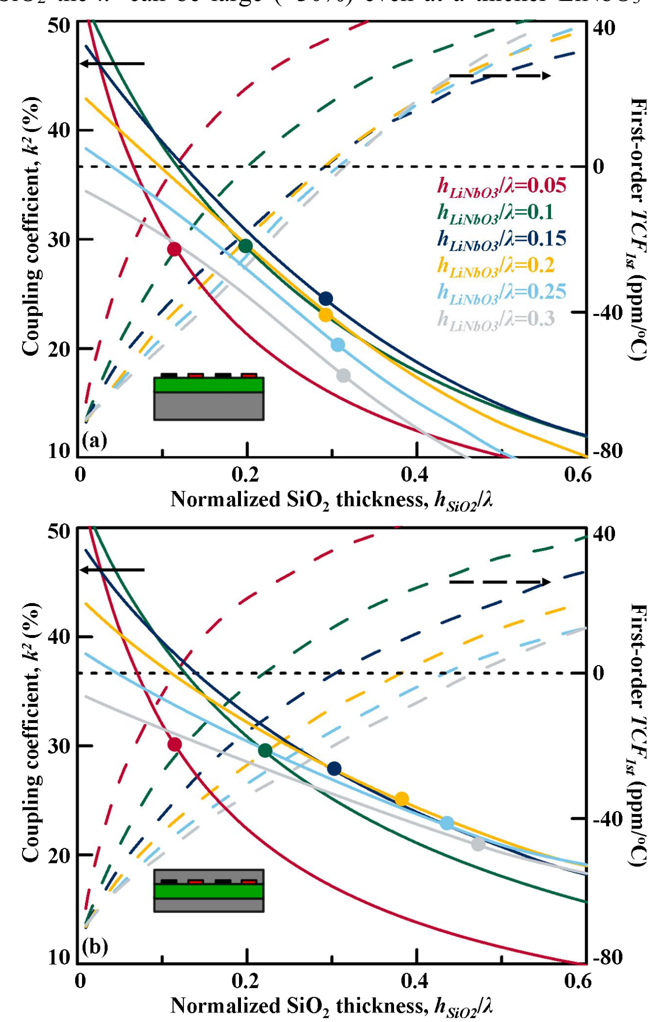

Fig. 5 Trade-off between the first-order TCF_{1st} and intrinsic k^2 of the SH_0 mode in the $LiNbO_3/SiO_2$ bi-layer structure and symmetrical $SiO_2/LiNbO_3/SiO_2$ composite membrane with single-IDT transducer.

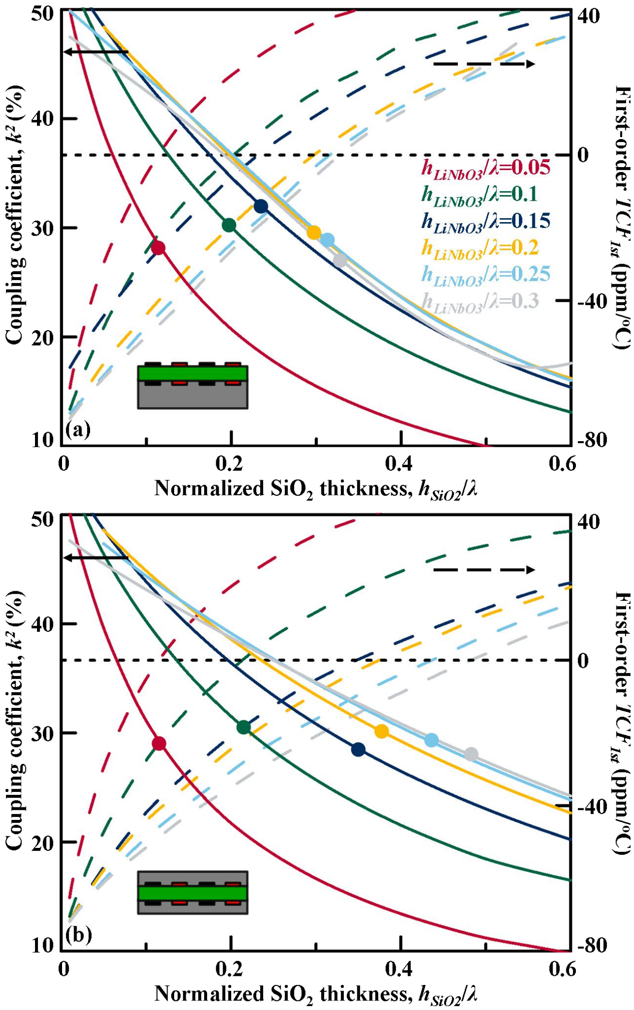

Fig. 6. Trade-off between the first-order *TCF* and intrinsic k^2 of the SH_0 mode in the $LiNbO_3/SiO_2$ bi-layer structure and symmetrical $SiO_2/LiNbO_3/SiO_2$ composite membrane with double-IDT transducer.

zero-*TCF*, showing potential for the multi-frequency application (large pitch variation in the same stack).

D. Dispersion

The periodically perturbed dispersion of the SH_0 wave propagating in $LiNbO_3$ membrane determined by the presence of a frequency stopband [8] will be impacted by adding the SiO_2 layer. The open-circuited (OC) dispersion analysis of the SH_0 wave travelling in the $LiNbO_3/SiO_2$ bilayer structure with near-zero *TCF* (h_{LiNbO3}/λ = 0.1 and h_{SiO2}/λ = 0.2) is provided in Fig. 7. For the OC boundary condition, the non-excited modes appear in the lower stopband edge when IDT is relatively thin (h_{IDT}/λ = 4% and h_{IDT}/λ = 6%) and start to be at the upper stopband edge when the IDTs become thicker (h_{IDT}/λ > 6%).The phenomenon of the non-excited mode below the OC excitable mode (f_p) is rare and detrimental to the passband performance. In this case, the short-circuited (SC) reflection coefficient is not enough to cover the OC excitable mode, and the OC reflection coefficient is negative. As a result, it is critical to use thicker IDT electrodes for the SH_0 resonators.

IV. CONCLUSIONS

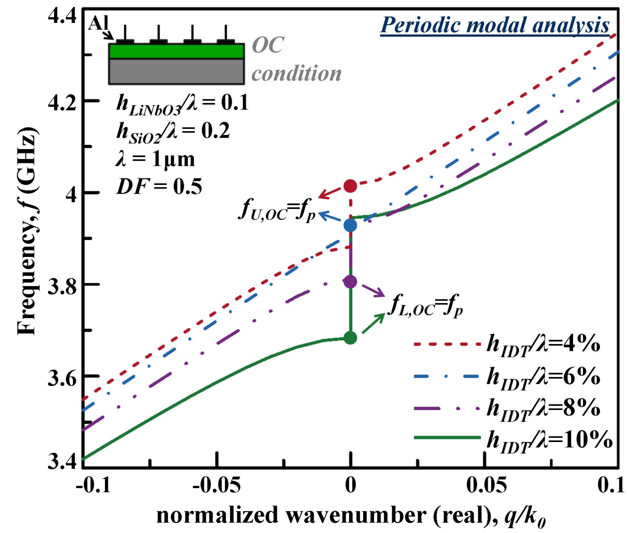

Fig. 7. Real part of the SH_0 propagation constant in single-IDT and open-circuited condition for different electrode thicknesses of the SH_0 mode propagating in the $LiNbO_3/SiO_2$ bilayer structure assuming λ = 1µm, h_{LiNbO3}/λ = 0.1, h_{SiO2}/λ = 0.2 and *DF* = 0.5.

The thermal stabilization techniques for the SH_0 mode in $LiNbO_3$ PAW resonators is investigated using the $LiNbO_3/SiO_2$ and $SiO_2/LiNbO_3/SiO_2$ structures. The $SiO_2/LiNbO_3/SiO_2$ sandwiched membrane enables higher v_p and larger k^2 than the $LiNbO_3/SiO_2$ bilayer since the symmetric structure traps more acoustic field in the $LiNbO_3$ piezoelectric layer. By considering the trade-off between *TCF* and k^2, simplest zero-*TCF* stack is proposed as $LiNbO_3/SiO_2$ with h_{LiNbO3}/λ = 0.1, h_{SiO2}/λ = 0.2, and single-IDT. The dispersive stopband analysis is given for this structure and the threshold IDT thickness of 8% is provided for wide enough stopband *BW* covering passband. Intriguingly, the $SiO_2/LiNbO_3/SiO_2$ structure with double-IDTs offers a wide selection of thickness combinations for simultaneously enabling large k^2 and zero-*TCF*, showing potential for the multi-frequency applications.

REFERENCES

[1] M. Kadota, Y. Kuratani, T. Kimura, M. Esashi1, and S. Tanaka, "Ultra-wideband and high frequency resonators using shear horizontal type plate wave in LiNbO3 thin plate," *Jpn. J. Appl. Phys.*, vol. 53, 07KD03, June 2014.

[2] M. Kadota and S. Tanaka, "Ultra-wideband ladder filter using SH0 plate wave in Thin $LiNbO_3$ plate and its application to tunable filter," *IEEE Trans Ultrason Ferroelectr Freq Control*, vol. 62, May. 2015.

[3] J. Zou, F. Iliev, R. B. Hammond, V. Plessky, S. Samadian, P. J. Turner, V. Yantchev, and N. O. Fenzi, "Design of Ultra-Large-Coupling SH_0 Plate Wave Resonators on $LiNbO_3$ with Clean Spectrum," *in IEEE Intl. Freq. Control Symp. (IFCS'19),* Orlando, FL, USA, May 2019.

[4] V. Plessky, S. Yandrapalli, P.J. Turner, L.G. Villanueva, J. Koskela and R.B. Hammond, "5 GHz laterally-excited bulk-wave resonators (XBARs) based on thin platelets of lithium niobate," *Electronics Letters*, vol. 55, Nov. 2018.

[5] M.-H. Li, R. Lu, Y. Yang, T. Wu, and S. Gong, "Temperature Stability Analysis of Thin-Film Lithium Niobate SH0 Plate Wave Resonators," *J. Microelectromech. Syst.*, early access.

[6] J. Zou, C.-M. Lin, A. Gao, and A. P. Pisano, "The multi-mode resonance in AlN Lamb wave resonators," *J. Microelectromech. Syst.*, vol. 27, issue 6, pp. 973-984, Dec. 2018.

[7] R. T. Smith and F. S. Welsh, "Temperature dependence of the elastic, piezoelectric and dielectric constants of Lithium Tantalate and Lithium Niobate," *J. Appl. Phys.*, vol. 42, pp. 2219–2230, May 1971.

[8] V. Yantchev, "Coupling-of-Modes Analysis of Thin Film Plate Acoustic Wave Resonators Utilizing the S0 Lamb Mode," *Trans Ultrason Ferroelectr Freq Control*, vol. 57, Apr. 2010.